International Journal of Energy Research

INTERNATIONAL JOURNAL OF ENERGY RESEARCH
Int. J. Energy Res. 2012; **36**:1366–1374
Published online 9 September 2011 in Wiley Online Library (wileyonlinelibrary.com). DOI: 10.1002/er.1918

The plasma focus—trending into the future

S Lee[1,2,3,*,†] and S H Saw[1,2]

[1]INTI International University, 71800 Nilai, Malaysia
[2]Institute for Plasma Focus Studies, 32 Oakpark Drive, Chadstone VIC3148, Australia
[3]Nanyang Technological University, National Institute of Education, Singapore, 637616

SUMMARY

The plasma focus is a promising small-scale alternative to the huge Tokamak project in the development of nuclear fusion energy. Its strength lies in the characteristic that the plasma condition is the same whether the plasma focus is a small sub-kilojoule machine or a large one with thousands of kilojoules of stored energy and the related constancy of the dynamic resistance. Yet, this strength turns out to result in a weakness. The observed neutron 'saturation' is more correctly stated as a 'scaling deterioration' effect. This critical weakness is due to the same constancy of the plasma condition intimately related to a constancy of the dynamic resistance. The understanding of this situation points to a new class of plasma focus devices to overcome the 'saturation' of the electric current. Plasma focus technology has to move to ultra high voltage technology and take advantage of circuit manipulation techniques in order to move into a new era of high performance. This paper examines fundamental scaling properties of the plasma focus including speeds, temperatures, dimensions and times. It links up these basic scaling characteristics with the crucial ideas of the inherent yield scaling deterioration, thus providing a clear understanding of its overall performance characteristics, paving the way for future exploitation. Copyright © 2011 John Wiley & Sons, Ltd.

KEY WORDS

plasma focus; nuclear fusion; plasma focus scaling; plasma focus properties; neutron saturation; new plasma focus devices

Correspondence

*Lee, Sing, Principal, IPFS,
[†]E-mail: leesing@optusnet.com.au

Received 26 February 2011; Revised 29 April 2011; Accepted 11 July 2011

1. INTRODUCTION

The plasma focus is one of the smaller scale devices which complement the international efforts to build a nuclear fusion reactor [1]. It is an important device for the generation of intense multiradiation including X-rays, particle beams and fusion neutrons. The physics underlying the mechanisms for the generation of these radiations in the plasma focus is still not completely known although there have been intensive investigations for the past five decades. Experimental and theoretical work on the focus has reached quite high levels. For example, detailed simulation, work on the plasma focus had been carried out since 1971 [2], and a large range of devices has been constructed from less than 100J small focus to greater than 1MJ large focus [3]. Advanced experiments have been carried out on the dynamics, radiation, instabilities and nonlinear phenomena [4]. Yet, despite all these intensive studies, very little regarding scaling appears to be documented with the exception of the scaling law for neutron yield. Other more recent work has thrown much needed light on other aspects of scaling such as how the dimensions of the dense focused plasma (the focus pinch) and the pinch lifetime scale with apparatus dimensions, the dominating dimension being the anode radius [5].

2. NEUTRON SCALING WITH ENERGY

Historically, the most appealing quantity for use as the base for scaling is the stored energy used to drive the focus. Using the highest voltage technologically convenient, all one needs to do to scale up energy ($E_0=0.5C_0V_0^2$) is to put in more capacitors in parallel, thus increasing the capacitance of the energy bank and incidentally also decreasing the static inductance L_0 of the bank to some extent. Thus, this has become a major preoccupation of the larger laboratories, sometimes seemingly at the expense of other considerations. Along these lines, early work has shown that the neutron yield $Y_n \sim E_0^2$, and since under ideal conditions (minimized inductance L_0 and when the system is dominated by the generator impedance), the capacitor current I may have the relationship $I \sim E^{0.5}$, then it quickly follows that $Y_n \sim I^4$. This very simplistic view has been too

smug and has led to the hold-up of the progress of large plasma focus devices. It was found that when the capacitor bank reached storage energies of only several hundred kJ, the neutron yield no longer increased, the so-called neutron saturation effect. It has been shown recently that whilst the discharge circuit is indeed dominated by the generator impedance at low energies, i.e. low capacitance so that indeed $I \sim E^{0.5}$, at a certain point when the C_0, i.e. E_0 gets sufficiently big, the generator impedance has dropped to such low values as to reach the value of the load impedance that the generator is driving. As E_0 is increased even further and further, the generator impedance eventually becomes negligible when compared to the load impedance which remains relatively constant, hardly affected by the decreasing generator impedance. Eventually, at very large E_0, the constant load impedance completely dominates, and the circuit current reaches an asymptotic value and does not even increase at all for a further increase in E_0 at those already very large values. At this point, typically in the high tens of MJ for the plasma focus, the capacitor current may be considered to have saturated, leading to neutron saturation. What is observed at hundreds of kJ and which has been termed as neutron saturation is based on very limited data. When more data from more experiments are put in together with data from rigorous systematic numerical experiments, then the global picture shows the scaling deterioration very clearly (see Figure 1). We will come back to this central problem again in the concluding section of this paper.

3. SCALING PROPERTIES OF THE PLASMA FOCUS

3.1. Various plasma focus devices

In Figure 2a is shown the UNU ICTP (United Nations University/ International Centre for Theoretical Physics) PFF 3 kJ device [6] mounted on a 1 m by 1 m by 0.5 m trolley, which was wheeled around the ICTP for the 1991 and 1993 Plasma Physics Colleges. The single capacitor is seen in the picture mounted on the trolley. In contrast, Figure 2b shows the 300-times larger PF1000, the 1 MJ device at the ICDMP in Warsaw Poland [7]. Only the chamber and the cables connecting the plasma focus to the capacitors are shown. The capacitor bank with its 288 capacitors, switches and chargers are located in a separate hall.

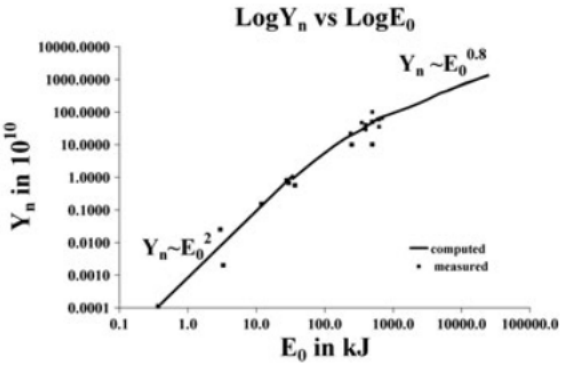

Figure 1. The global scaling law, combining experimental and numerical data. The global data illustrates Y_n scaling observed in numerical experiments from 0.4 kJ to 25 MJ (solid line) using the Lee model code, compared to measurements compiled from publications (squares) of various machines from 0.4 kJ to 1 MJ.

We show in Table I the characteristics of three plasma focus devices [8] computed using the Lee model code, fitted by comparing the computed current waveform to the measured current waveform. These computed characteristics are also in broad agreement with measured experimental values where available in the published literature [6,7,9].

In Table I, we look at the PF1000 and study its properties at typical operation with device storage at 500 kJ level. We compare this big focus with two small devices at the kJ level.

From Table I, we note:

Voltage and pressure do not have any particular relationship to E_0.

Peak current I_{peak} increases with E_0.

Anode radius 'a' increases with E_0.

Current per cm of anode radius (ID) I_{peak}/a is in a narrow range 160 to 210 kA/cm

SF (speed or drive factor) $(I_{peak}/a)/P_0^{0.5}$ is 82 to 100 (kA/cm) torr$^{0.5}$deuterium gas. Observed peak axial speed v_a is in the narrow range 9 to 11 cm/us.

Fusion neutron yield Y_n ranges from 10^6 for the smallest device to 10^{11} for the PF1000.

We stress that whereas the ID and SF are practically constant at around 180 kA/cm and 90 (kA/cm) per torr$^{0.5}$ deuterium gas throughout the range of small to big devices, Y_n changes over five orders of magnitude.

We emphasise that the data of Table I is generated from numerical experiments, and most of the data has been confirmed by actual experimental measurements and observation.

Table II compares further the properties of the range of plasma focus devices. The properties being compared in this table are mainly related to the radial phase. These are computed from numerical experiments and found to be in close agreement with laboratory measurements [5,10].

The pinch temperature T_{pinch} is strongly correlated to the square of the radial pinch speed v_p.v_p itself is closely correlated to the value of v_a and c=b/a, so that for a constant v_a, v_p is almost proportional to the value of c [11].

Notably, the dimensions and lifetime of the focus pinch scales as the anode radius 'a'.

r_{min}/a (almost constant at 0.14–0.17)z_{max}/a (almost constant at 1.5)

Pinch duration has a relatively narrow range of 8–14 ns/cm of anode radius.

The duration per unit anode radius is correlated to the inverse of T_{pinch}.

T_{pinch} itself is a measure of the energy per unit mass. It is quite remarkable that this energy density at the focus pinch varies so little (factor of 5) over a range of device energy of more than three orders of magnitude (factor of 1000).

a b

Figure 2. (a) 3kJ UNU ICTP PFF. (b) 1MJ PF1000 plasma focus.

Table I. Scaling properties of the plasma focus.

	E_0	a	z_0	V_0	P_0	I_{peak}	v_a	ID	SF	Y_n
	kJ	cm	cm	kV	Torr	kA	cm/μs	kA/cm	(kA/cm) $torr^{0.5}$	10^8
PF1000	486	11.6	60	27	4	1850	11	160	85	1100
UNU ICTP	2.7	1.0	15.5	14	3	164	9	173	100	0.20
PF-400J	0.4	0.6	1.7	28	7	126	9	210	82	0.01

Table II. Scaling properties of the plasma focus in radial phase.

	c=b/a	a	T_{pinch}	v_p	r_{min}	z_{max}	Pinchduration	r_{min}/a	z_{max}/a	Pinch duration/a
		cm	10^6K	cm/μs	cm	cm	ns			ns/cm
PF1000	1.4	11.6	2	13	2.2	19	165	0.17	1.6	14
UNU ICTP PFF	3.4	1.0	8	26	0.13	1.4	7.3	0.14	1.4	8
PF400J	2.6	0.6	6	23	0.09	0.8	5.2	0.14	1.4	9

This practically constant pinch energy density (per unit mass) is related to the constancy of the axial speed moderated by the effect of the values of c=b/a on the radial speed.

The constancy of r_{min}/a suggests that the devices also produce the same compression of ambient density to maximum pinch density, with the ratio (maximum pinch density)/(ambient density) being proportional to $(a/r_{min})^2$. Hence, for two devices of different sizes starting with the same ambient fill density, the maximum pinch density would be the same.

From the above discussion, we may put down as rule-of-thumb the following scaling relationships, subject to minor variations caused primarily by the variation in c.

Axial phase energy density (per unit mass)	constant
Radial phase energy density (per unit mass)	constant
Pinch radius ratio	constant
Pinch length ratio	constant
Pinch duration per unit anode radius	constant

Summarizing, the dense hot plasma pinch of a small E_0 plasma focus and that of a big E_0 plasma focus have essentially the same energy density, the same mass density. The big E_0 plasma focus has a bigger physical size and a bigger discharge current. The size of the plasma pinch scales proportionately to the current and to the anode radius, as does the duration of the plasma pinch. The bigger E_0, the bigger I_{peak}, the bigger 'a' has to be, hence the larger the plasma pinch and the longer the duration of the plasma pinch. The larger size and longer duration of the big E_0 plasma pinch are essentially the properties leading to the bigger

Int. J. Energy Res. 2012; **36**:1366–1374 © 2011 John Wiley & Sons, Ltd.
DOI: 10.1002/er

neutron yield compared to the yield of the small E_0 plasma focus.

We may also summarize the dimensions and lifetimes for deuterium and neon plasma focus pinch in Table III as follows [5,10]:

Table III. Dimensions and durations of the plasma focus.

		Deuterium	Neon (for SXR)
minimum radius	r_{min}	0.15a	0.05a
max length (hollow anode)	z	1.5a	1.6a
radial shock transit	t_{comp}	5×10^{-6}a	4×10^{-6}a
pinch lifetime	t_p	10^{-6}a	10^{-6}a
speed factor	SF	90	

where, for the times in s, the value of anode radius, a, is in m. For the neon calculations, radiative terms are included, and the stronger compression (smaller radius) is due to thermodynamic effects. The units of the speed factor SF are: (kA/cm)/(torr$^{0.5}$).

The above description of the plasma focus combines data from numerical experiments, consistent with laboratory observations [5,8,10,11].

The next section describes briefly the code.

4. INTRODUCTION TO THE LEE MODEL CODE

The Lee model code couples the electrical circuit with plasma focus dynamics, thermodynamics and radiation, enabling a realistic simulation of all gross focus properties. The basic model, described in 1984 [12], was successfully used to assist several projects [6,13,14]. Radiation-coupled dynamics was included in the five-phase code, leading to numerical experiments on radiation cooling [15]. The vital role of a finite small disturbance speed discussed by Potter in a *Z*-pinch situation [16] was incorporated together with real gas thermodynamics and radiation-yield terms. This version of the code assisted other research projects [17–22] and was web published in 2000 [23] and 2005 [24]. Plasma self-absorption was included in 2007 [23], improving the SXR yield simulation. The code has been used extensively in several machines including UNU/ICTP PFF [6,15,17,19–22,25], NX2 [18,26,27] and NX1 [27,28] and has been adapted for the Filippov-type plasma focus DENA [29]. A recent development is the inclusion of the neutron yield Y_n using a beam–target mechanism [30–34], incorporated in recent versions [8,11] of the code (versions later than RADPFV5.13), resulting in realistic Y_n scaling with I_{pinch} [30,31]. The versatility and utility of the model are demonstrated in its clear distinction of I_{pinch} from I_{peak} [32] and the recent uncovering of a plasma focus pinch current limitation effect [33–36], as static inductance is reduced towards zero. Extensive numerical experiments had been carried out systematically resulting in the uncovering of neutron [1,30,31,37–39] and SXR [40–43] scaling laws over a wider range of energies and currents than attempted before. The numerical experiments also gave insight into the nature and cause of 'neutron saturation' [31,38,44]. The description, theory, code and a broad range of results of this "Universal Plasma Focus Laboratory Facility" are available for download from [8,11].

A brief description of the five-phase model is given in the following.

4.1. The five phases

The five phases (*a–e*) are summarized [11,35,38,45,46] as follows:

a. *Axial Phase (see Figure 3 left part)*

Described by a snowplow model with an equation of motion which is coupled to a circuit equation. The equation of motion incorporates the axial phase model parameters: mass and current factors f_m and f_c. The mass swept-up factor [47] f_m accounts for not only the porosity of the current sheet but also for the inclination of the moving current sheetshock front structure, boundary layer

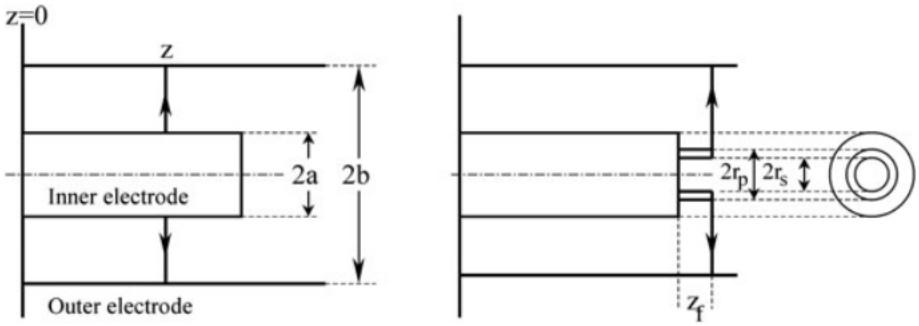

Figure 3. Schematic of the axial and radial phases. The left section depicts the axial phase, the right section the radial phase. In the left section, z is the effective position of the current sheath-shock front structure. In the right section, r_s is the position of the inward moving shock front driven by the piston at position r_p. Between r_s and r_p is the radially imploding slug, elongating with a length z_f. The capacitor, static inductance and switch powering the plasma focus are shown for the axial phase schematic only.

effects and all other unspecified effects which have effects equivalent to increasing or reducing the amount of mass in the moving structure, during the axial phase. The current factor f_c accounts for the fraction of current effectively flowing in the moving structure (due to all effects such as current shedding at or near the back-wall, and current sheet inclination). This defines the fraction of current effectively driving the structure, during the axial phase.

b. *Radial Inward Shock Phase (see Figure 3 right part, also Figure 4)*

Described by four coupled equations using an elongating slug model. The first equation computes the radial inward shock speed from the driving magnetic pressure. The second equation computes the axial elongation speed of the column. The third equation computes the speed of the current sheath, (magnetic piston), allowing the current sheath to separate from the shock front by applying an adiabatic approximation [16]. The fourth is the circuit equation. Thermodynamic effects due to ionization and excitation are incorporated into these equations, these effects being particularly important for gases other than hydrogen and deuterium. Temperature and number densities are computed during this phase using shock-jump equations. A communication delay between shock front and current sheath due to the finite small disturbance speed [11,16,46] is crucially implemented in this phase. The model parameters, radial phase mass swept-up and current factors f_{mr} and f_{cr} are incorporated in all three radial phases. The mass swept-up factor f_{mr} accounts for all mechanisms which have effects equivalent to increasing or reducing the amount of mass in the moving slug, during the radial phase. The current factor f_{cr} accounts for the fraction of current effectively flowing in the moving piston forming the back of the slug (due to all effects). This defines the fraction of current effectively driving the radial slug.

c. *Radial Reflected Shock (RS) Phase (See Figure 4)*

When the shock front hits the axis, because the focus plasma is collisional, a RS develops which moves radially outwards, while the radial current sheath piston continues to move inwards. Four coupled equations are also used to describe this phase, these being for the RS moving radially outwards, the piston moving radially inwards, the elongation of the annular column and the circuit. The same model parameters f_{mr} and f_{cr} are used as in the previous radial phase. The plasma temperature behind the RS undergoes a jump by a factor close to 2. Number densities are also computed using the RS jump equations.

d. *Slow Compression (Quiescent) or Pinch Phase (See Figure 4)*

When the outgoing RS hits the inward moving piston, the compression enters a radiative phase in which for gases such as neon, radiation emission may actually enhance the compression where we have included energy loss/gain terms from Joule heating and radiation losses into the piston equation of motion. Three coupled equations describe this phase; these being the piston radial motion equation, the pinch column elongation equation and the circuit equation, incorporating the same model parameters as in the previous two phases. The duration of this slow compression phase is set as the time of transit of small disturbances across the pinched plasma column. The computation of this phase is terminated at the end of this duration.

e. Expanded Column Phase

To simulate the current trace beyond this point, we allow the column to suddenly attain the radius of the anode and use the expanded column inductance for further integration. In this final phase, the snow plow model is used, and two coupled equations are used similar to the axial phase above. This phase is not considered important as it occurs after the focus pinch.

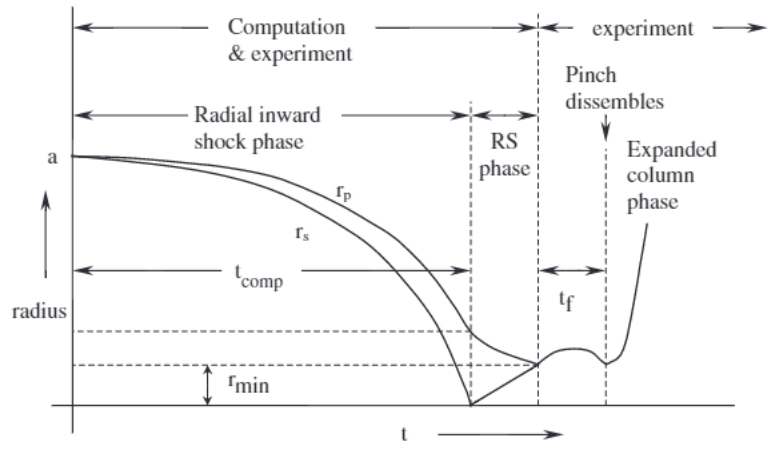

Figure 4. Schematic of radius versus time trajectories to illustrate the radial inward shock phase when r_s moves radially inwards, the reflected shock (RS) phase when the RS moves radially outwards, until it hits the incoming piston r_p leading to the start of the pinch phase (t_f) and finally the expanded column phase.

Int. J. Energy Res. 2012; **36**:1366–1374 © 2011 John Wiley & Sons, Ltd.
DOI: 10.1002/er

We note [45] that in radial phases *b*, *c* and *d*, axial acceleration and ejection of mass caused by necking curvatures of the pinching current sheath result in time-dependent strongly center-peaked density distributions. Moreover, the transition from phase *d* to phase *e* is observed in laboratory measurements to occur in an extremely short time with plasma/current disruptions resulting in localized regions of high densities and temperatures [48]. These center-peaking density effects and localized regions are not modeled in the code, which consequently computes only an average uniform density and an average uniform temperature which are considerably lower than measured peak density and temperature. However, because the four model parameters are obtained by fitting the computed total current waveform to the measured total current waveform, the model incorporates the energy and mass balances equivalent, at least in the gross sense, to all the processes which are not even specifically modeled. Hence, the computed gross features such as speeds and trajectories and integrated soft X-ray yields have been extensively tested in numerical experiments for several machines and are found to be comparable with measured values.

4.2. The model code as a general diagnostic tool

The model code now includes a sheet in which is displayed charts of the properties of the particular shot including: total discharge current and plasma current, tube voltage, axial trajectories and speeds, tube inductance and total inductive energy, piston work and Joule work related to the dynamic resistance, the dynamic resistance, ion and electron number density (spatial uniform averaged and peak), plasma temperature (spatial uniform averaged and peak), computed soft X-ray power; all these properties are displayed as functions of time, in the axial phase (where applicable) and in the radial phase. The model code thus provides information to guide experimental measurements and in this sense can be considered as a powerful diagnostics tool as well [38].

5. NEUTRON SATURATION—ITS RELATIONSHIP WITH THE PLASMA FOCUS PROPERTIES

In Section 2, we had discussed the global scaling law for neutron yield as shown in Figure 1 which was compiled with data from experiments and numerical experiments. Figure 1 shows that whereas at energies up to tens of kJ the $Y_n \sim E_0^2$ scaling held, deterioration of this scaling became apparent above the low hundreds of kJ. This deteriorating trend worsened and tended towards $Y_n \sim E_0^{0.8}$ at tens of MJ. The global data of Figure 1 suggests that the apparently observed neutron saturation effect is overall not in significant variance with the deterioration of the scaling shown by the numerical experiments.

5.1. The cause of neutron 'saturation' is the dynamic resistance

A simple yet compelling analysis of the cause of this neutron saturation has been published [31,44]. In that paper [44], it is shown that it is the interaction of dynamic resistance of the plasma focus axial phase with the generator impedance of the plasma focus capacitor bank that causes the deterioration of the scaling trend and eventual saturation of yield at high multi-MJ energies. This dynamic resistance is practically a constant over the range of plasma focus devices, depending as it is on the value of ln(c) (where radius ratio c=b/a) and on the axial speed; the latter being practically a constant, and the c having only a small range typically from 1.5 to 3. The value of this dynamic resistance is typically 5 mΩ. The value of the generator impedance of the capacitor bank on the other hand is $Z_0 = (L_0/C_0)^{0.5}$, inversely proportional to $C_0^{0.5}$ and is much larger than the dynamic resistance for small plasma focus while being much smaller than the dynamic resistance for large plasma focus devices as C_0 is increased from the range of μF to the range of tens of thousands of μF. It turns out that in the region of kJ to tens of kJ, the scaling of the current is controlled by the bank impedance. In this range of energy, the current thus increases with $C_0^{0.5}$. On the other hand, at very large MJ energies, the capacitor bank impedance has dropped so much below the dynamic resistance that the circuit current is now controlled solely by the dynamic resistance. As this is a constant, increasing the capacitance or bank energy any further no longer affects the circuit current which then tends to an asymptotic value. The point at which the current scaling begins to deteriorate is in the range of low hundreds of kJ. As bank energy increases to this range of energies, the scaling of current begins to deteriorate; the deterioration worsens as MJ levels are approached, but it is not until the high tens of MJ that circuit current begins to approach saturation. Likewise, the behavior of the neutron yield. Thus, the term neutron 'saturation' popularly referred to in the literature at several hundred kJ is a misnomer, mistakenly applied to what is in fact just a neutron yield scaling deterioration.

The asymptotic value at high tens of MJ is $I_{peak} = V_0/Z_{total} \sim V_0/DR_0$ where V_0 is charging voltage, Z_{total} is total circuit impedance which tends towards the value of the axial phase dynamic resistance DR_0 since at very large values of C_0, the value of $Z_0 = (L_0/C_0)^{0.5} << DR_0$. Thus, DR_0 causes current 'saturation'. This is shown in Figure 5.

In other extensive numerical experiments, we had shown the following relationships between Y_n and I_{peak} and I_{pinch} as follows:

$$Y_n \sim I_{pinch}^{4.5} \quad (1)$$

$$Y_n \sim I_{peak}^{3.8} \quad (2)$$

Hence, saturation of I_{peak} will lead to saturation of Y_n.

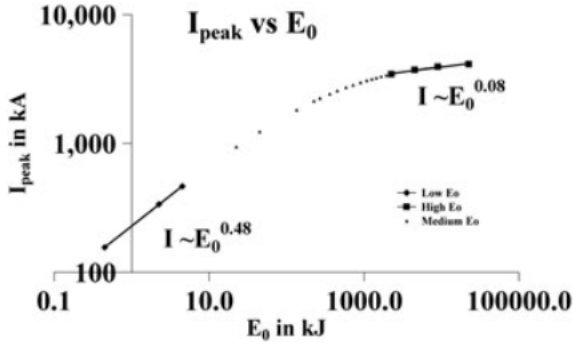

Figure 5. I_{peak} versus E_0 on log-log scale, illustrating I_{peak} 'saturation' at large E_0

Thus, we have shown that neutron 'saturation' is inevitable as E_0 is increased to very large values by an increase in C_0, simply due to the dominance of the axial phase dynamic resistance. However, the apparently observed neutron 'saturation' at low hundreds of kJ is more accurately represented as a neutron scaling deterioration.

5.2. Relationship with plasma focus scaling properties

Now, we link up this neutron scaling law deterioration and subsequent saturation with the scaling properties of the plasma focus discussed in Section 3. This scaling law deterioration and saturation is due to the constancy of the speed factor SF and energy density, as E_0 increases. The constancy of the axial speed or SF caused the deterioration of current scaling, requiring that the anode radius 'a' is not increased as much as it would have been increased if there were no deterioration. This implies that the size and duration of the focus pinch are also restricted by the scaling deterioration. Ultimately, at high tens of MJ, I_{peak} saturates, the anode radius of the focus should not be increased anymore with E_0. The size and duration of the focus pinch no longer increase with E_0, and Y_n also saturates. We now have the complete picture.

6. CONCLUSIONS

This paper has reviewed the global scaling law for neutron yield as a function of storage energy. First, the scaling deterioration and eventual 'saturation' of circuit current are ascribed to the energy density constancy manifested in the form of a constancy in dynamic resistance of the axial phase. Second, the deterioration of current scaling implies that the anode radius 'a' is not increased as much as it would have been if there were no deterioration. Third, this implies that the size and duration of the focus pinch are also restricted by the scaling deterioration. Ultimately at high tens of MJ, I_{peak} saturates, the anode radius of the focus should not be increased anymore with E_0, the size and duration of the focus pinch no longer increase with E_0.

The restriction on the plasma pinch size and duration has a corresponding effect on the neutron yield Y_n. The neutron yield Y_n scales with E_0^2 at low energies up to tens of kJ, begins to exhibit scaling deterioration around low hundreds of kJ and approaches 'saturation' at high tens of MJ.

In this manner, this paper has for the first time connected the global scaling laws for the current and the neutron yield to the scaling properties of the plasma focus. This more complete picture will facilitate the further development of the plasma focus as a fusion device.

The understanding of this situation points to a new class of plasma focus devices to overcome the 'saturation' of the electric current. Plasma focus technology has to move to ultra high voltage technology and take advantage of circuit manipulation techniques [31,38,44,49–51] in order to move into a new era of high performance.

REFERENCES

1. Lee S. Nuclear fusion and the Plasma Focus. Invited paper Tubav Conferences: Nuclear & Renewable Energy Sources Ankara, Turkey, 28 & 29 September 2009. Procs:pg 9–18
2. Potter DE. *Numerical Studies of the Plasma Focus Physics Fluids* 1971; **14**:1911–1914.
3. Soto L. New trends and future perspectives on plasma focus research. *Plasma Physics and Controlled Fusion* 2005; **47**:A361.
4. Bernard A, Bruzzone H, Choi P, Chuaqui H, Gribkov V, Herrera J, Hirano K, Krejci A, Lee S, Luo C, *et al.* Scientific Status of Plasma focus Research. *Moscow Journl Physical Society* 1998; **8**:93–170.
5. Lee S, Serban A. "Dimensions and lifetime of the plasma focus pinch". *IEEE Trans. Plasma Sci.* 1996; **24**(3):1101–1105.
6. Lee S, Tou TY, Moo SP, Eissa MA, Gholap AV, Kwek KH, Mulyodrono S, Smith AJ, Suryadi S, Usada W,.

Zakaullah M. A simple facility for the teaching of plasma dynamics and plasma nuclear fusion. *Amer. J. Phys.* 1988; **56**(1):62–68.
7. Gribkov VA, Banaszak A, Bienkowska B, Dubrovsky AV, Ivanova-Stanik I, Jakubowski L, Karpinski L, Miklaszewski RA, Paduch M, Sadowski MJ, Scholz M, Szydlowski A, Tomaszewski K. Plasma dynamics in the PF-1000 device under fullscale energy storage: II. Fast electron and ion characteristics versus neutron emission parameters and gun optimization perspectives. *J. Phys. D Appl. Phys.* 2007; **40**(12):3592–3607.
8. Web-site: http://www.intimal.edu.my/school/fas/UFLF/ 2010.
9. Silva P, Moreno J, Soto L, Birstein L, Mayer RE, Kies W. *Applied Physics Letters* 2003; **83**:3269.
10. Lee S. *Characterising the Plasma Focus Pinch and Speed Enhancing the Neutron Yield*. In First Cairo Conference on Plasma Physics & Applications. 11–15 October 2004. International Cooperation Bilateral Seminars (Vol **34**). Forschungszentrum Juelich GmbH, Juelich, Germany, pp.27–33. ISBN 3-89336-374-2
11. Lee S. Radiative Dense Plasma Focus Computation Package: RADPF. http://www.plasmafocus.net. http://www.plasmafocus.net/IPFS/modelpackage/File1RADPF.htm. http://www.plasmafocus.net/IPFS/modelpackage/File2Theory.pdf. http://www.plasmafocus.net/IPFS/modelpackage/UPF.htm. 2010.
12. Lee S. Plasma focus model yielding trajectory and structure. In *Radiations in Plasmas*, McNamara B (Ed.). World Scientific: Singapore, 1984; **II**:978–987.
13. Tou TY, Lee S, Kwek KH. Non perturbing plasma focus measurements in the run-down phase. *IEEE Trans. Plasma Sci.* 1989; **17**(2):311–315.
14. Lee S. A sequential plasma focus. *IEEE Trans. Plasma Sci.* 1991; **19**(5):912–919.
15. Ali J. Development and studies of a small plasma focus, Ph.D. Dissertation; Universiti Teknologi Malaysia, Malaysia, 1990.
16. Potter DE. The formation of high-density z-pinches. *Nuclear Fusion.* 1978; **18**:813–823.
17. Liu M. Soft X-rays from compact plasma focus, Ph.D. dissertation, NIE, Nanyang Technological Univ., Singapore, 2006. ICTP Open Access Archive. [Online]. Available: http://eprints.ictp.it/327/
18. Bing S. Plasma dynamics and X-ray emission of the plasma focus, Ph.D. dissertation, NIE, Nanyang Technological Univ., Singapore, 2000. ICTP Open Access Archive. [Online]. Available: http://eprints.ictp.it/99/
19. Serban A. Lee S. Experiments on speed-enhanced neutron yield from a small plasma focus. *Journal of Plasma Physics* 1998; **60**(1):pt. 1, 3–15, Aug. 1998.
20. Liu MH, Feng XP, Springham SV, Lee S. Soft X-ray measurement in a small plasma focus operated in neon. *IEEE Trans. Plasma Sci.* 1998; **26**(2):135–140.
21. Lee S. in Twelve Years of UNU/ICTP PFF—A Review. Trieste, Italy: Abdus Salam ICTP, 1998, pp. 5–34. IC/ 98/ 231, ICTP Open Access Archive. [Online]. Available: http://eprints.ictp.it/31/
22. Springham SV, Lee S, Rafique MS. Correlated deuteron energy spectra and neutron yield for a 3kJ plasma focus. *Plasma Physics and Controlled Fusion* 2000; **42**(10):1023–1032.
23. Lee S. 2010. [Online]. Available: http://ckplee.myplace.nie.edu.sg/plasmaphysics/
24. Lee S. ICTP Open Access Archive, 2005. [Online]. Available: http://eprints.ictp.it/85/
25. Mohammadi MA, Sobhanian S, Wong CS, Lee S, Lee P, Rawat RS. The effect of anode shape on neon soft X-ray emissions and current sheath configuration in plasma focus device. *J. Phys. D, Appl. Phys.* 2009; **42**(4):10. 045 203.
26. Wong D, Lee P, Zhang T, Patran A, Tan TL, Rawat RS, Lee S. An improved radiative plasma focus model calibrated for neonfilled NX2 using a tapered anode. *Plasma Sources Sci. Technol.* 2007; **16**(1):116–123.
27. Lee S, Lee P, Zhang G, Feng X, Gribkov VA, Liu M, Serban A, Wong T. High rep rate high performance plasma focus as a powerful radiation source. *IEEE Trans. Plasma Sci.* 1998; **26**(4):1119–1126.
28. Bogolyubov EP, Bochkov VD, Veretennikov VA, Vekhoreva LT, Gribkov VA, Dubrovskii AV, Ivanov YP, Isakov AI, Krokhin ON, Lee P, Lee S, Nikulin VY, Serban A, Silin PV, Feng X, Zhang GX. A powerful soft X-ray source for X-ray lithography based on plasma focusing. *Physica Scripta* 1998; **57**(4):488–494.
29. Siahpoush V, Tafreshi MA, Sobhanian S, Khorram S. Adaptation of Sing Lee's model to the Filippov type plasma focus geometry. *Plasma Physics and Controlled Fusion* 2005; **47**(7):1065–1075.
30. Lee S, Saw SH. Neutron scaling laws from numerical experiments. *J. Fusion Energy* 2008; **27**(4):292–295.
31. Lee S. Current and neutron scaling for megajoule plasma focus machines. *Plasma Physics and Controlled Fusion* 2008; **50**(10):14. 105 005.
32. Lee S, Saw SH, Lee PCK, Rawat RS, Schmidt H. Computing plasma focus pinch current from total current measurement. *Applied Physics Letters* 2008; **92**(11):111 501.
33. Lee S, Saw SH. Pinch current limitation effect in plasma focus. *Applied Physics Letters* 2008; **92**(2):021 503.
34. Lee S, Lee P, Saw SH, Rawat RS. Numerical experiments on plasma focus pinch current limitation. *Plasma Physics and Controlled Fusion* 2008; **50**(6):8. 065 012.

35. Internet Workshop on Plasma Focus Numerical Experiments (IPFS-IBC1) 14 April-19 May 2008 http://www.plasmafocus.net/IPFS/Papers/IWPCAkey-note2ResultsofInternet- basedWorkshop.doc
36. Akel M, Al-Hawat S, Lee S. Pinch Current and Soft x-ray yield limitation by numerical experiments on Nitrogen Plasma Focus. *J Fusion Energy* 2010; **29**:94.
37. Saw SH, Lee S. Scaling laws for plasma focus machines from numerical experiments. Invited paper: IWPDA, Singapore 2&3 July 2009
38. Lee S. Diagnostics and Insights from Current waveform and Modelling of Plasma Focus. Keynote address: IWPDA, Singapore 2-July 2009
39. Saw SH, Lee S. Scaling the plasma focus for fusion energy considerations. Tubav Conferences: Nuclear & Renewable Energy Sources, Ankara, Turkey, 28 & 29 September 2009.
40. Lee S, Saw SH, Lee P, Rawat RS. Numerical Experiments on Neon plasma focus soft x-rays scaling. *Plasma Physics and Controlled Fusion* 2009; **51**:8.105013.
41. Akel M, Al-Hawat S, Lee S. Numerical Experiments on Soft X-ray Emission Optimization of Nitrogen Plasma in 3kJ Plasma Focus SY-1 Using Modified Lee Model. *J Fusion Energy* DOI 10.1007/s10894-009-9203-4 First online, May 19, 2009.
42. Akel M, Al-Hawat S, Saw SH, Lee S. Numerical Experiments on Oxygen Soft X-Ray Emissionsfrom Low Energy Plasma Focus Using Lee Model. *J Fusion Energy* 2010; **29**:223–231.
43. Lee S, Rawat RS, Lee P, Saw SH. Soft x-ray yield from NX2 plasma focus. *JOURNAL OF APPLIED PHYSICS* 2009; **106**:023309.
44. Lee S. "Neutron Yield Saturation in Plasma Focus-A fundamental cause". *APPLIED PHYSICS LETTERS* 2009; **95**:151503 published online 15 October 2009
45. Saw SH, Lee PCK, Rawat RS, Lee S. Optimizing UNU/ICTP PFF Plasma Focus for Neon Soft X-ray Operation. *IEEE Trans on Plasma Sc* 2009; **37**:1276–1282.
46. Lee S, Saw SH, Soto L, Moo SP, Springham SV. Numerical experiments on plasma focus neutron yield versus pressure compared with laboratory experiments. *Plasma Physics and Controlled Fusion* 2009; **51**:11. 075006.
47. Chow SP, Lee S, Tan BC. Current sheath studies in a co-axial plasma focus gun. *J Plasma Phys* 1972; **8**:71.
48. Favre M, Lee S, Moo SP, Wong CS. X-ray emission in a small plasma focus operating with H2-Ar mixtures. *Plasma Sources Science and Technology* 1992; **1**:122–125.
49. Lee S, Saw SH. Numerical Experiments providing new Insights into Plasma Focus Fusion Devices. *Invited Review Paper: Special edition on "Fusion Energy" Energies* 2010; **3**:711–737.
50. Saw SH. Experimental studies of a current-stepped pinch. PhD Thesis Universiti Malaya, Malaysia, 1991.
51. Lee S. A current-stepping technique to enhance pinch compression. *J Phys D: Appl Phys* 1984; **17**:733–741.